Studying microstructure of heat-resistant alloy based on the Fe-Cr-Ni-alloying element system for manufacture of components for metallurgical equipment

Sv. S. Kvon, *Cand. Eng., Prof.* [1], *e-mail: svetlana.1311@mail.ru;*
V. Yu. Kulikov, *Cand. Eng.* [1], *Prof.;*
S. K. Arinova, *Ph. D., Lecturer* [1], *e-mail: sanya_kazah@mail.ru;*
E. P. Shcherbakova, *Ph. D., Senior Lecturer* [1], *e-mail: sherbakova_1984@mail.ru*

[1] *Karaganda Technical University (Karaganda, Kazakhstan)*

The paper presents the results of studying the microstructure and phase composition of an experimental heat-resistant alloy based on the Fe-Cr-Ni-alloying element system intended for manufacturing of components for metallurgical equipment. Samples of an experimental alloy were prepared for research. Electron microscopy using X-ray mapping was used as a research method. X-ray phase analysis was performed to verify the phase identification. Influence of alloying elements on formation of intermetallic strengthening phases in an experimental alloy is considered. It is shown that the alloy matrix is represented by a γ-solution by the type of substitution and interstitial phases of Ni_3Al, MeC. The existence of a new intermetallic phase Me_2B, identified taking into account the chemical composition of the alloy, as $(Nb, Mo)_2B$, has been identified and experimentally proved. This phase is represented by significantly smaller inclusions. Microstructural and X-ray spectral analysis of the samples confirmed the presence of the above phases. It has been shown that the presence of this phase in the structure has a positive effect on the value of longterm strength. Furnace roller tables were cast from smelted experimental steel in normal operation.
Key words: heat resistance, microstructure, micro-X-ray spectral analysis, intermetallic phase, longterm strength, creep limit, alloying, fine structure.
DOI: 10.17580/cisisr.2023.01.14

Introduction

A significant part of the furnace equipment (rollers, pallets, grates, furnace accessories, etc.) in the metallurgical and foundry industries is made of heat-resistant steels, which is associated with the peculiarities of operating conditions: high temperatures, constant load and duration of use. The operation of products at high temperatures and under the action of constant loading leads to the development of creep with subsequent destruction [1-5].

At present in the CIS countries, most of the furnace equipment components are made of heat-resistant steels of the 20Kh25N20S2, 35Kh18N24S2L grades. The durability of the components made of these steels is low and makes 3-4 months in average, then it is necessary to replace them, which leads to equipment downtime and reduced productivity. The reason for the short life of the parts is relatively low heat resistance of steels they are made of [6-10]. An alternative to heat-resistant steels are heat-resistant alloys based on Cr-Ni or Ni-Co systems. These alloys have high heat resistance but they also have a high cost, which does not justify their use in this case [11-15].

Based on the thermodynamic calculation using the ThermoCalc software (Sweden) and laboratory experiments, the composition of a heat-resistant alloy based on the Fe–Cr–Ni-alloying element system was proposed (**Table 1**) [16, 17]. A distinctive feature of this alloy, compared to other alloys based on Cr-Ni or Ni-Co systems, is Fe introduction into the composition of the alloy. In the case of nimonics, the presence of iron in the alloy is an undesirable impurity, since it leads to decreasing heat resisting properties. In this case, the introduction of iron in the alloy makes it possible to reduce the cost in comparison with pure Cr-Ni or Ni-Co alloys; decreasing heat resistance is partially compensated by the introduction of other alloying elements. It should be emphasized that in this case the goal is not to achieve in the new alloy the same heat resistance indicators as in Cr-Ni or Ni-Co alloys, because the experimental alloy is designed for products operating under milder temperature and loading conditions. The experimental alloy shows fairly good parameters of longterm strength, which suggests the possibility of its use for manufacturing parts. In order to more accurately predict the properties of the alloy, its microstructure has been studied.

The aim of this research is to study the fine structure of an experimental heat-resistant alloy based on the Fe-Cr--alloying element system.

The authors express their gratitude to D. R. Aubakirov, a doctoral student, senior lecturer of the Department of Nanotechnology and Metallurgy, for participating in this work.

Materials and methods

An experimental heat-resistant alloy has been used as an object of study. The melts have been carried out in an induction furnace UI-25p with an improved cooling system, in a corundum-mullite-zirconium crucible. Then the melt has been poured into molds, the mass of ingots was 200-300 g. The chemical composition of the obtained alloy has been monitored using a Poly Spec-F spectrometer. The chemical composition of the obtained alloy was monitored using a Polyspek-F spectrometer. The analysis was carried out at 3 points in different parts of the sample, the data spread was no more than 10 %. The composition of the smelted alloy is shown in **Table 1**.

After cooling, the samples have been subjected to heat treatment, consisting of quenching from 1100 °C in oil, followed by aging during 4 hours at 700 °C and cooling in air.

The tests for longterm strength and creep have been carried out on a TRMP-50-E testing machine. The test samples were made of a cylindrical shape with a diameter of 5 mm and a length of 25 mm according to GOST 10145-81. Longterm strength has been determined at the preset bending (UBS) and bending angle (γ). These characteristics are highly correlated with standard tensile properties (UBS ≈ 1,7*UTS, MPa and γ (degrees) ≈ 4*El, %).

To study the fine structure of the test samples, there has been used an S-3400N scanning electron microscope equipped with a NORAN X-ray energy dispersion spectrometer of the Hitachi High-Technologies Corporation.

The qualitative and quantitative phase composition of the test samples has been determined using X-ray diffraction analysis on an X-PertPRO X-ray diffractometer. The sensor computer is equipped with the DIFFRAC plus SEARCH database, using which the data results have been processed, which made it possible to unambiguously diagnose the phases.

X-ray studies were carried out on the X'PertPRO diffractometer using CuKα radiation. Accelerating voltage makes 30 kV, current is equal to 10 mA, a nickel filter was used. The diffraction spectrum was taken from 5 to 120 degrees of Bragg angles. Focusing of the goniometer was done according to the Bragg-Brentano scheme. The experimental spectra were processed using the diffractometer software: X'Pert High Score Plus version 2.2b and X'Pert High Score version 2.2b.

Results and discussion

Table 2 shows the data of longterm strength and creep strength of the test alloy sample. Heat-resistant steel 20Kh25N20S2 has been used as a reference sample, as it is most widely used at the works of the Republic of Kazakhstan.

Analysis of the obtained results shows that the parameters of the heat-resistant properties of the test alloy at the temperature of 900 °C are approximately 30 % higher than those of steel 20Kh25N20S2. At the temperature of 1000 °C, the reference sample has been destroyed.

It is obvious that presence of heat-resistant properties determines the phase and structural composition of the alloy stipulated by its chemical composition. As it is shown in works [18, 19], heat-resistant alloys can contain phases that strengthen the dispersion γ'-phases, and secondary phases that are $\gamma + \gamma'$ eutectic, and eutectoid carbides of the $M_{23}C_6$ type (complex cubic carbide), as well as TDP (topological densely-packed) phases, Laves phases and an undesirable σ–phase.

Using X-ray microanalysis, a map of the distribution of elements at different points in the structure has been obtained (**Fig. 1**).

Table 3 presents the data of the element composition at different points of the structure.

It can be seen from the data in **Table 3** that most of the spectra are presented by rather homogeneous composition: Ni content is within the range 23.6-31.9 %; Cr content is within the range 18.5-20.2 %, etc., i.e. the microspectral analysis data correspond well with the data of the chemical composition of the alloy in the Table 1. Fig. 1*b* shows the general picture of the elements distribution in the alloy. Based on the data in Table 3, we can conclude that the main part of the alloying elements is localized in the matrix, forming a solid solution by the type of substitution with the exception of carbon (**Fig. 2*c***).

Table 1. **Chemical composition of the experimental alloy**

	Elements								
No	C	Ni	Cr	Al	Mo	Nb	Co	B	Fe
1	0,07	37	18	2,5	1,1	2,5	18,5	1,0	ост.

Table 2. **Heat-resistant characteristics of the test alloy**

Samples	Longterm strength, MPa, at the temperature, ⁰C, during 50 hours			Creep strength, MPa, at the temperature,⁰C, with 3% deformation during 50 hours	
	800	900	1000	800	1000
Reference sample (20Kh25N20S2)	197	196	-	89	-
Test alloy	349	280	235	110	62

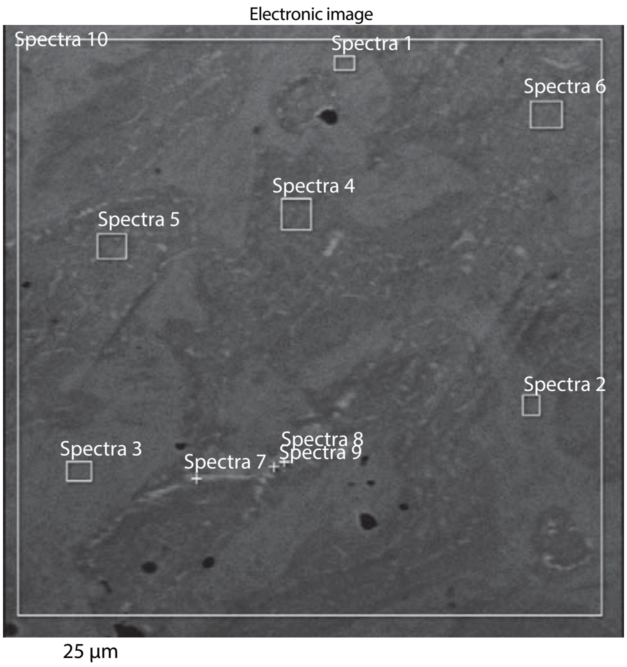

a

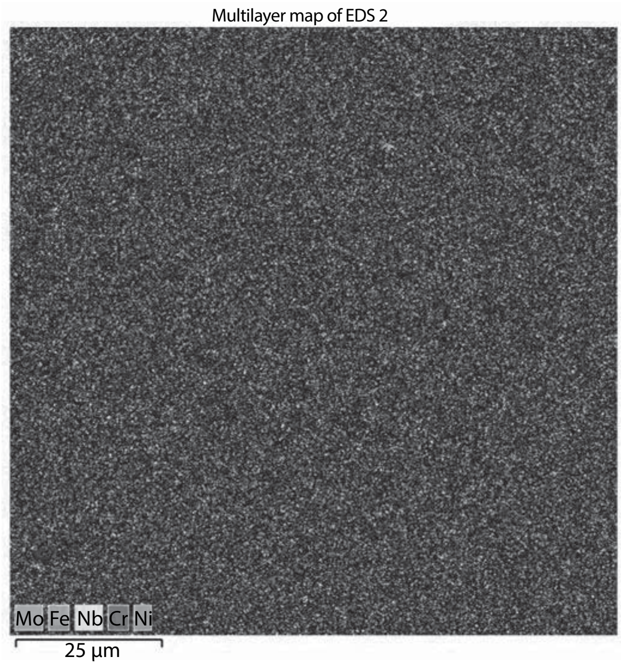

b

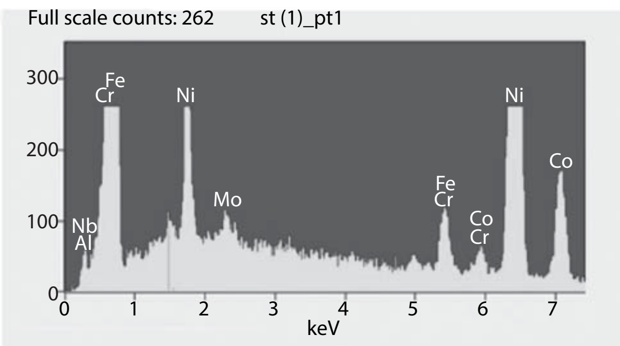

c

Fig. 1. X-ray microanalysis results:
a – X-ray microanalysis regions in the sample structure;
b – general picture of the elements distribution;
c – characteristic spectrum of the matrix (points *1-4*)

Table 3. **Concentration of chemical elements in the selected spectrum, % (mass.)**

Spectra	Concentration of the alloy component in the selected spectrum, %, (mass.)								
	Ni	Cr	Fe	Mo	Al	Nb	B	Co	C
1	28.1	18.5	29.00	1.13	2.8	1.65	0.65	18.1	0.062
2	31.9	18.44	25.8	1.0	2.6	1.60	0.59	18.0	0.05
3	23.6	18.55	35.02	1.31	2.9	1.51	0.58	16.5	0.03
4	31.2	19.30	25.2	1.48	2.5	1.74	0.84	17.6	0.065
5	30.9	20.01	24.9	1.22	2.4	1.56	0.76	18.1	0.071
6	31.6	19.40	27.36	1.32	2.4	1.50	0.56	15.8	0.061
7	29.3	18.62	19.90	4.33	3.0	3.84	4.45	16.5	0.058
8	30.1	20.20	21.22	3.33	2.7	3.89	3.49	15.0	0.073
9	28.3	19.06	22.50	3.57	2.6	3.8	3.00	17.1	0.068
10	29,1	18,42	27,76	1,46	2,4	1,8	0,70	18,3	0,054

The exception and, accordingly, the most interesting aspects are presented in the spectra 7, 8 and 9. It can be seen from the data in Table 3 that these spectra are characterized by the increased content of Mo, Nb, and B. If the content of these elements in the remaining spectra is about 1 %, 1.5 %, and 0.5 % on average, respectively, then in spectra 7–9 content of these elements increases by 2–4 times.

For example, the Mo content in spectrum 7 is 4.33 % compared with the background content 1.2 %. The Nb content in the same spectrum is 3.84 % compared with the

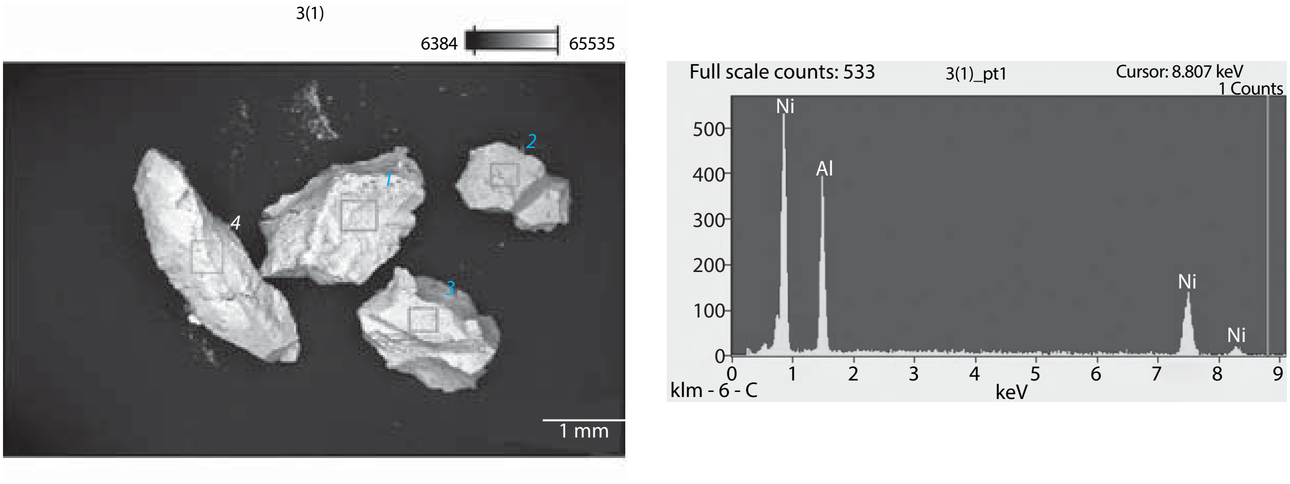

a *b*

Fig. 2. X-ray microanalysis results for the interstitial phases in the points of localization:
a – the point of sampling; *b* – characteristic view of the X-ray spectrum at the point *3*

Table 4. **Concentration of chemical elements in the selected analyzed spectrum, % (mass.)**

Spectra	Element content, % (mass.)							∑
	Al-K	Ni-K	Cr-K	Nb-K	Co-K	Fe-K	Mo-K	
1	2.2	28.1	15.3	2.2	11.6	39.6	1.0	100
2	2.9	27.9	15.4	2.9	11.0	38.5	1.4	100
3	2.6	28.7	15.8	2.6	11.3	37.4	1.6	100

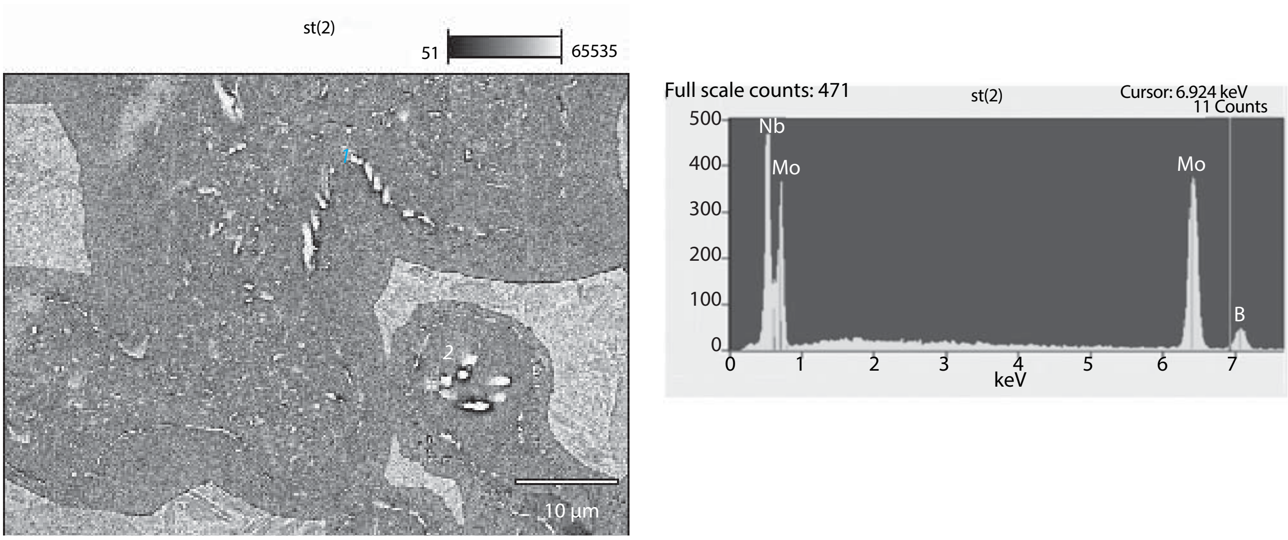

a *b*

Fig. 3. X-ray microanalysis results for the interstitial phases with the new interstitial phase:
a – the point of sampling; *b* – characteristic view of the X-ray spectrum at the point *3*

background content 1.65 %. The content of B in spectrum 7 increases to 4.45 % compared with the background content 0.65 %. If we compare the data of Table 2 with the places of reflection of the spectra (see Fig. 1), then it can be seen that spectra 7–9 fall on the interstitial phases, in contrast to other spectra obtained from the matrix.

It is obvious that such elements as niobium, molybdenum, and boron form a new phase that is incoherent with the matrix and most likely has properties different from those of the matrix. To determine the nature of the interstitial phases, additional studies have been carried out using X-ray microanalysis at the points of localization of the interstitial phases (Fig. 2*a*).

Table 5. **Concentration of chemical elements in the selected analyzed spectrum. % (mass.)**				
Spectra	Element content, % (mass.)			Σ
	Nb-K	Mo-K	B-K	
1	41.95	45.95	12.1	100
2	42.3	46	11.7	100

Table 6. **Semi-quantitative X-ray phase analysis of crystalline phases results**					
No	D-spacing, A	Rel. Int., %	Compound	Chemical formula	Concentration, %
1	7.29719	8.88	Iron Nickel	Fe-Ni	45
2	2.02726	100	Boron, Niobium, Molybdenum	$(Nb, Mo)_2B$	11
3	1.17025	14.63	Nickel Aluminum	Ni_3Al	16
4	1.30501	2.75	Nickel	Ni	13
5	1.43193	7.15	Phase laves	AB_2	15

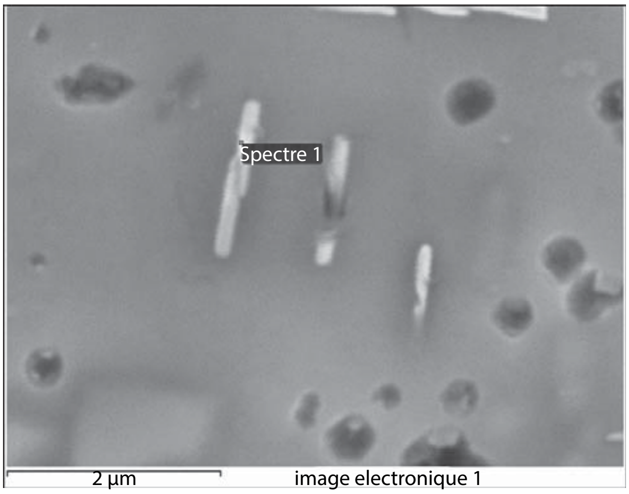

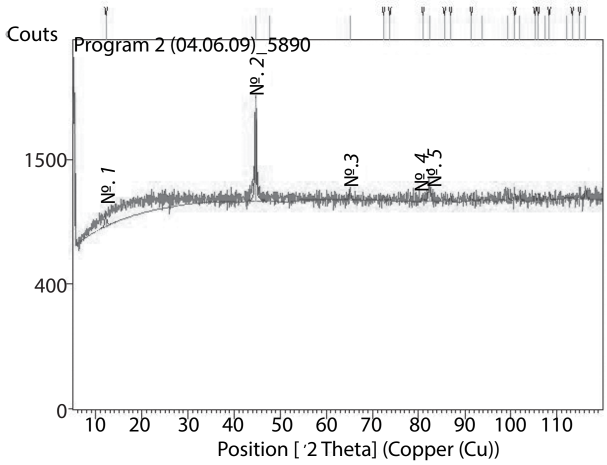

Fig. 4. X-ray diffractometry of the samples studied:
a — example of the spectrum localization; *b* — typical diffraction pattern

According to the results of the X-ray spectrum (Fig. 2*b*, **Table 4**), a strengthening γ'-phase of the Ni_3Al type has been revealed. This intermetallic compound is well studied and is one of the known hardening phases that determine the alloy longterm strength [20].

In addition to the indicated Ni_3Al phase and insignificant amount of the MeC type carbide phase, a new interstitial phase has been detected (**Fig. 3***a*) that has not been identified in any of the phases considered above. This phase is represented by much smaller inclusions localized along the grain boundaries of the main matrix. The analysis of the spectra (Fig. 3*b*, **Table 5**) shows the increased 1:1 ratio of niobium and molybdenum compared to the matrix, as well as presence of boron.

In addition to the other alloying elements, the experimental alloy contains such elements as Nb, Mo, and B. It was noted in work [21] that in presence of Group V metals and B in the Cr-Ni-based alloy, a new phase of the Me_2B type can be formed.

Based on the obtained data of the analysis and in this case, and taking into account the chemical composition of the alloy and elemental investigation of the phase, the latter can be identified as $(Nb, Mo)_2B$.

Formation of a new intermetallic phase $(Nb, Mo)_2B$ allows explaining the hardening mechanism of the testing alloy. Its matrix is represented by alloyed austenite-type solution with a sufficiently coarse grain. High tensile strength is ensured by the presence of such phases as Ni_3Al and MeC type carbides. Formation of a new intermetallic phase of the $(Nb, Mo)_2B$ type leads to increasing the ultimate strength in comparison with the standard since this phase has higher hardness and is stable, like all borides, to high temperatures; it is also localized along the grain boundaries of the matrix. All these factors, according to the generally accepted theory of alloying heat-resistant alloys, provide increasing the alloy ultimate strength, which has been experimentally confirmed [19-21].

X-ray phase analysis of the samples confirmed presence of identifiable interstitial phases (**Table 6**, **Fig. 4**).

The comparative analysis of the obtained X-ray diffraction patterns of the experimental samples with the database shows high phase content with the FCC lattice identified as γ-solution based on Fe-Ni (peak 1); the presence of the Ni_3Al phase (peak 2), as well as the presence of a new phase (peak 3), which is identified as the Me_2B type phase.

Comparison the chemical analysis data of spectra 7–9 and the XRD data confirms the correctness of identification of the interstitial phase as $(Nb, Mo)_2B$.

Conclusion

Thus, the studies show that in the structure of the experimental heat-resistant alloy based on the Fe-Cr-Ni system, additionally alloyed with Mo, Nb and B, there is also a new phase identified as $(Nb, Mo)_2B$ in addition to the well-known γ-matrix by the type of substitution, and the known Ni_3Al phase and MeC type carbides. This phase has not been experimentally observed previously. The phase is incoherent with the matrix and apparently has a significant effect on the hardening mechanism, since the ultimate strength increases in its presence.

Furnace rollers were cast from the smelted experimental steel and installed in a thermal furnace for normal operation. The next stage of research will be to study the structural changes in the experimental steel in real operation. The estimated service life is 3,500 hours.

Acknowledgments

This research has been is funded by the Science Committee of the Ministry of Education and Science of the Republic of Kazakhstan AP09058350 «Developing and implementing the technology of producing chrome anti-friction cast iron for components of mining equipment».

REFERENCES

1. Konovalov S., Ivanov Y., Gromov V., Panchenko I. Fatigue-induced evolution of AISI 310S steel microstructure after electron beam treatment. *Materials*. 2020. Iss. 13 (20). No. 4567. pp. 1-13. DOI: 10.3390/ma13204567.
2. Bai X., Han Y., Liaw P. K., Wei L. Effect of Ion Irradiation on Surface Microstructure and Nano-Hardness of SA508-IV Reactor Pressure Vessel Steel. *Journal of Materials Engineering and Performance*. 2022. Vol. 31 (3). pp. 1981-1990. DOI: 10.1007/s11665-021-06376-x.
3. Xu Haoran, Han Kai, Li Meng. Sandwich-like polythioetherimide-decorated polypropylene (Celgard2400) composite separators with heat resistance and wettability for safety lithium-ion batteries. *International journal of electrochemical science*. 2020. Vol. 15. Iss. 1. pp. 788-802.
4. Dmitriyeva H. P., Cherepova T. S., Kosorukova T. A. Effect of Rhenium on the Heat Resistance of the Alloy of Cobalt with Niobium Carbide. *Materials science*. 2019. Vol. 55. Iss. 2. pp. 181-186.
5. Wang Jie, Yu Zixin, Li Peihua. Poly (styrene-rancinnamic acid) (SCA), an approach to modified polystyrene with enhanced impact toughness, heat resistance and melt strength. *RSC advances*. 2019. Vol. 9. Iss. 68. pp. 39631-39639.
6. Dzyura V., Maruschak P. Optimizing the formation of hydraulic cylinder surfaces, taking into account their microrelief topography analyzed during different operations. *Machines*. 2021. Vol. 9 (6). No. 116. DOI: 10.3390/machines9060116.
7. Goldstein M. I., Grachev S. V., Veksler Yu. G. Special steels. M.: Metallurgiya. 2009. 320 p.
8. Hiroaki M., Teruhiko F., Chieko F. Magnetic properties and microstructures of high-Fe and low-Zr heat-resistant Sm-Co Magnets. *64th Annual Conference on Magnetism and Magnetic Materials (MMM)*. Las Vegas, Nevada. November 04-08, 2019. 125042-1-5.
9. Yanyan P., Liming Y., Yongchang L. Microstructures and tensile properties of an austenitic ODS heat resistance steel. *Materials science and engineering α-structural materials properties microstructure and processing*. 2019. Vol. 767. No. 138419.
10. Terentieva V. S., Astapov A. N., Rabinskiy L. N. State in the field of heat-resistant coatings for heat-proof nickel alloys and steels. *Periodico tche quimica*. 2019. Vol. 16. Iss. 33. pp. 561-572.
11. Kozlov E. V., Nikonenko E. L., Popova N. A., Koneva N. A. Mechanisms of hardening heat-resistant alloys based on nickel. *Fundamental Problems of Modern Materials Science*. 2016. No. 1. pp. 39-42.
12. Xiaotao L., Wenbin L., Lijuan M., Junling L., Jing L. Effect of boron on the microstructure, phase assemblage and wear properties of Al0.5CoCrCuFeNi High-Entropy Alloy. *Rare Metal Materials and Engineering*. 2016. Vol. 45. No. 9. pp. 2201-2207.
13. Xiang S., Chen X., Fan Z.,, Lia X. A deep learning-aided prediction approach for creep rupture time of Fe–Cr–Ni heat-resistant alloys by integrating textual and visual features. *Journal of Materials Research and Technology*. 2022. Vol. 18. pp. 268-281.
14. Nabiran N., Weber S., Theisena W. Influence of intermetallic precipitates and heat treatment on the mechanical properties of high-temperature corrosion resistant ferritic steels. *Procedia Engineering*. 2011. Vol. 10. pp. 1651-165.
15. Weimin G., Xiaotian Zh., Hongyu Zh., Xiaofeng S., Qi Zh. Melting of primary carbides in a cobalt-base superalloy. *Journal of Alloys and Compounds*. 2019. No. 787. pp. 152-157.
16. Zhang H. W.,Wu Y. S., Qin X. Z., Zhou L. Z., Li X. W. Microstructures and high-temperature mechanical properties of a directionally solidified Ni-based superalloy: Influence of boron content. *Journal of Alloys and Compounds*. 2018, October 30. Vol. 767. pp. 915-923.
17. Ducki K. J. Analysis of the Precipitation and Growth Processes of the Intermetallic Phases in an Fe-Ni superalloy. *Intech open science, superalloys,* 2015. pp.112-139.
18. Kulikov V. Yu., Issagulov A. Z., Kvon Sv. S. Studying the effect of boron on heat-resistance properties of Ni-Cr alloys. *Metalurgija*. 2017. Vol. 56. Iss. 3-4. pp. 409-411.
19. Kvon Sv., Issagulov A., Kulikov V., Medvedeva I., Arinova S. Studying heat treatment impact on heat resisting properties of Cr-Ni-a.e. system alloy. *Metalurgija*. 2017. Vol. 56.. Iss. 3-4. pp. 382-384.
20. Kvon Sv. S., Kulikov V. Yu., Issagulov A. Z. Studying structure and properties of shaped ingots obtained in various conditions of crystallization. *Metalurgija*. 2018. Vol. 57. Iss. 4. pp. 313-316.
21. Kvon Sv. S., Kulikov V. Yu., Shcherbakova Ye. P. Effect of inoculant introducing on improving ingot structure. *Metalurgija*. 2019. Vol. 58. Iss. 3-4. pp. 315-318.